Journal of
Water & Climate Change

IWA PUBLISHING

Journal of Water and Climate Change Vol 15 No 9, 4405 doi: 10.2166/wcc.2024.106

Is the rate of extremely climate-intensifying rainfall for Bangkok severely propagating into flooding?

Apin Worawiwat and Chavalit Chaleeraktrakoon*

Department of Civil Engineering, Faculty of Engineering, Thammasat University (Rangsit Campus), Klong Luang, Pathumthani, Thailand
*Corresponding author. E-mail: cchava@engr.tu.ac.th

AW, 0000-0002-9094-726X; CC, 0000-0003-1398-8727

ABSTRACT

The present paper assesses whether the extremely climate-intensifying rate (i.e., 14%/°C) for maximum rainfall in Bangkok is severely propagating into flooding. The impact evaluation involves the development of a flooding assessment method for a drainage system (DS) representative of the capital and the application of the developed procedure to assess the interested effect of the DS on its flooding. Considering the DS of Thammasat University (DS-TU) as the typical DS for the city, the popular storm water management model (SWMM) is then used for developing the dynamic simulation method against the most critical flooding condition of the DS-TU. Applying this SWMM for impact assessment of the intense rainfall rate has indicated that the rising temperature in excess of 2 °C would cause the gradient to severely propagate into the flooding because of the rapid increase in its associated peak, volume and duration properties. The propagated flooding has been shown to be further escalated, as a result of the clogging in the DS-TU. The clogging height that exceeded the 30% threshold of the full openings would intensify the volume and duration properties increasingly.

Key words: climate change impact, polder drainage, rainfall–runoff simulation model, urban flooding

HIGHLIGHTS

- The rising temperature limit that causes the flooding to be more severe than expected is found.
- Considering the common clogging problem in a drainage system is proposed for flooding assessment.

GRAPHICAL ABSTRACT

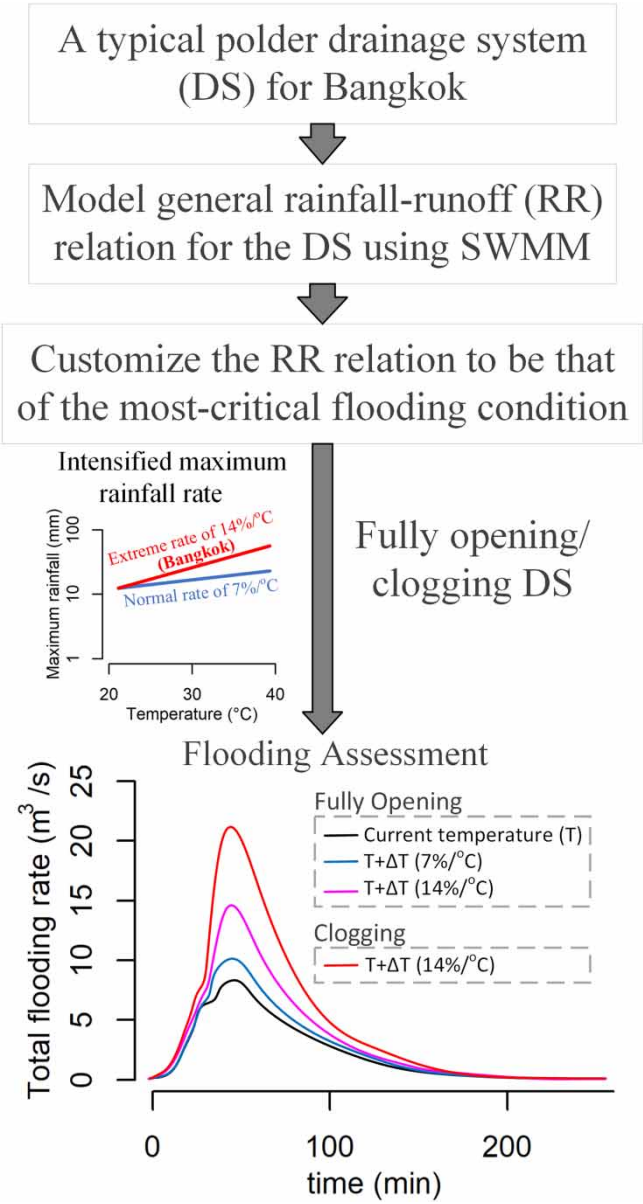

1. INTRODUCTION

Flooding in Bangkok is one of the serious problems that causes increasingly huge direct and indirect economical losses every year. Management of the total flooding by diversion of partially incoming upstream flood and construction of flood-control polder system (Saito 2014; BMA 2020; Kiguchi *et al.* 2021) has currently changed the inundation problem to be due mainly to only the maximum storm rainfall of the study capital. This principal rainfall–flooding connection consequently causes the city inundation to be greatly influenced by global warming impact through the climate-intensifying precipitation shown by many previous investigations (Nguyen *et al.* 2007; Wilby *et al.* 2009; Trenberth 2011; Arnbjerg-Nielsen *et al.* 2013; Ashish 2013; Wasko & Sharma 2015; Wibig & Piotrowski 2018; Hamilton *et al.* 2019; Nguyen & Nguyen 2020; Agarwal *et al.* 2023a, b).

Recently, the physical-based Clausius–Clapeyron (C–C) relationship between maximum rainfall and associated temperature (Trenberth 2011; Wasko & Sharma 2015; Wibig & Piotrowski 2018) has been used to assess the climate change impact on the precipitation for the city, and the analyzed C–C relation is found to be quite extreme (Worawiwat *et al.* 2021). The

increased scaling of the relation is almost double the normal 7%/°C rate that is usually used in most preceding studies on intensified flooding (Hettiarachchi *et al.* 2018; Alexander *et al.* 2019; Maimone *et al.* 2023). This, hence, raises an interesting question as to whether the extremely climate-intensifying rainfall is severely propagating via a drainage system (DS) into the city flooding.

Moreover, the intense climate impact on the flooding would be even more critical if the service level of the storm sewer system was considered. In particular, the continuous drain of runoff and wastewater flows under poor solid waste disposal in the capital causes a progressive increase in blockages of the DS. This steadily reduces the conveyance capacities of the system network and consequently increases the climate-related flooding. Although the explained clogging problem that additionally increases the climate effect is common (Qian *et al.* 2022; Quang *et al.* 2022), none of the preceding impact assessment studies for the city has, however, taken it into consideration.

Hence, the present paper develops a flooding assessment method for a DS representative in Bangkok and applies the developed procedure to evaluate the impact of the extremely increasing rainfall rate (i.e., 14%/°C) on the flooding of the typical DS. Among several different approaches available for forecasting and modeling flood flows (see, e.g., Niazi *et al.* 2017; Hettiarachchi *et al.* 2018; Zhou *et al.* 2018; Agarwal *et al.* 2021, 2022), the scheme of rainfall–runoff relation as the main cause and effect of the city flooding was then adopted for a modeling base when developing the assessment method in this study. Choosing the DS of Thammasat University, TU (Rangsit) to be a usual DS in the capital, its rainfall–runoff relationship for the most critical flooding condition in the DS-TU was then developed with the commonly used SWMM – i.e., storm water management model (Niazi *et al.* 2017). Application of the developed SWMM for the above-mentioned impact assessment has demonstrated that the rise in temperatures over 2 °C would bring about the propagation of the intense 14%/°C rate into severe flooding. In addition, it is also shown that the flooding of the extreme scaling would be further increased notably if the clogging in the DS-TU climbed over the 30% level of the fully opened condition.

2. METHOD

A method that could evaluate the impact of climate-intensifying rainfall on the most critical flooding via a typical DS for Bangkok has been developed in this section. Development of this assessment procedure composed of choosing the DS, building its general rainfall–runoff model and finding the condition for the most serious flooding in the system is briefly presented in the following.

2.1. A typical DS for Bangkok

Located 42 km north of Phahonyothin Road in the greater Bangkok area, the DS-TU enclosed by flood-control dykes was selected as a typical DS for the capital in this study. The chosen DS-TU possesses physical characteristics and soil types that are generally similar to those of most drainage networks used. Having been established in 1987, the DS-TU is responsible for the drainage of total wastewater and runoff flows over the whole TU area of 2.26 km^2. The DS has been continuously improved to meet the increase in the total flows, as a result of converting open and green spaces into impervious areas during the development of the university. Moreover, following the 2011 Great Thailand flood, it was then surrounded by flood-control dykes with a height from 2.5 to 3.0 m above ground level implemented for preventing the university from inundation in the neighbors.

Figure 1 schematically presents the current flood-control DS-TU that consists of a combination of storm sewers, ditches, canals, detention ponds and a pumping station. The slope of this system generally varies between 1:1,000 and 1:2,500. It starts collecting the wastewater and runoff flows of every sub-catchment into an associated storm sewer with a diameter ranging from 0.6 to 1.2 m. The pipe flows are then discharged into an appropriate rectangular or trapezoidal ditch of 0.8–1.0 m in depth and later drained into a trapezoidal canal with a depth varying from 1.5 to 3.5 m. Controlled by several detention ponds of 2.0–2.5 m in depth available, the canal discharges subsequently flow into the main canal along the north boundary of the DS-TU, prior to releasing them into the side drain of the road. Such local releases will be discharged freely if the surroundings are not flooded. Otherwise, they will be pumped out at a capacity of 2.0 m^3/s to secure the university from the local flooding.

2.2. Model development

A rainfall–runoff simulation model of the DS-TU has been formulated using the comprehensive SWMM software of the U.S. Environment Protection Agency (Niazi *et al.* 2017) that is freely downloaded via www.epa.gov/water-research/storm-water-management-model-swmm. Following the schematic DS-TU diagram in Figure 1, the formulation of the SWMM started with

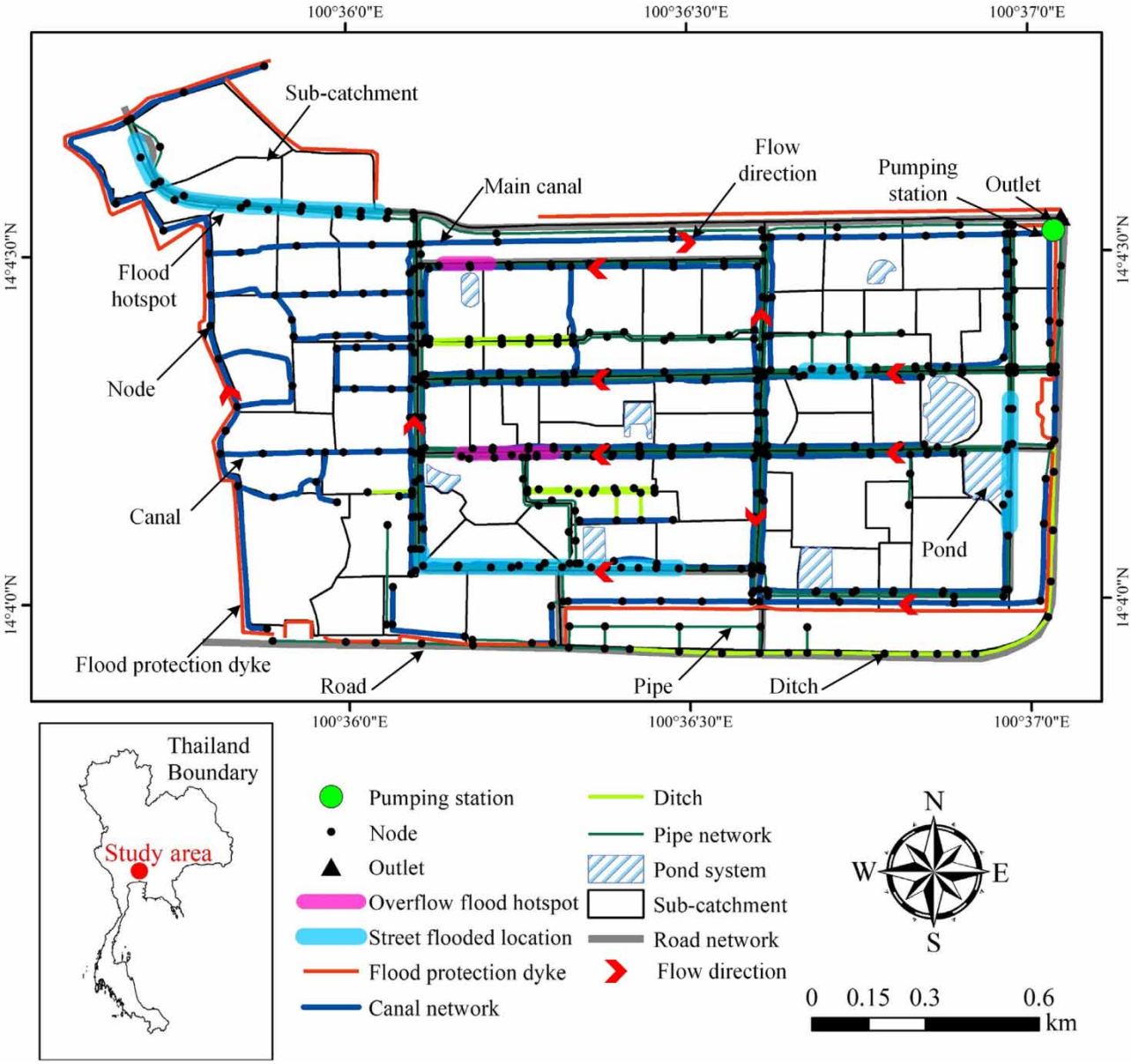

Figure 1 | Schematic diagram of the current flood-control DS-TU consisting of a combination of storm sewers, ditches, canals, detention ponds, dykes, roads and a pump station. *Note*: The drainage facilities are designed using the maximum flow for 25-year return period. See basic information for these facilities in Haruyama (1993), Eamathicom & Ounsiri (2011) and Kongprasert & Lekpungthiam (2013).

delineating the whole university area into 79 sub-areas (see the partitioned blocks in the figure) and then totally assigning 466 computational nodes for the system considered (see the black circle dots in the figure). The bed elevation of the appurtenant drainage structures was then evaluated using the LIDAR dataset in 2-m resolution of the Royal Irrigation Department, Thailand (non-officially published data) together with the necessary information of the DS.

Subsequently, the model establishment adopted the rainfall–runoff relation of the National Resources Conservation Service, previously well-known as the U.S. Department of Agriculture Soil Conservation Service (SCS), for explaining the infiltration loss of the sub-watersheds (Rossman & Huber 2016). Accordingly, using the SCS loss that depended mainly on a combination of land uses and soil types would enable the formulated SWMM to be applicable for the impact assessment of urbanization, one of the most important environmental changes in hydrology (Anuthaman *et al.* 2023). In this formulation, the rainfall losses expressed in terms of runoff curve numbers (i.e., lowest to highest imperviousness ranges from 0 to 100) for

all of the sub-areas were found to be between 79 and 98, provided that the underlying silty clay soil was type D (Haruyama 1993) and the land use information was taken from the appropriate Airbus satellite images in 2020 exported from Google Earth (Image ©2020 Airbus). Note that the level of soil moisture content was assumed to be normal.

Next, the Saint-Venant flow equations in one-dimensional form (Rossman 2017) were specified to simulate the flows in the DS-TU. Moreover, as they might be discharged gravitationally or reversely depending on a condition whether the surroundings were flooded or not, the accurate flow simulation of the SWMM was, hence, performed using the technique of fully dynamic wave routing. In addition, the pumping capacity for the DS-TU outflow was defined at the rate of 2 m^3/s, and the 2-m flow depth upstream of the system outlet was also set as the threshold to start pumping.

Further development of the formulated SWMM for the DS-TU was carried out to find Manning's roughness coefficient of its hydraulic conveyance structures. In practice, calibration and validation of the model are performed using observed available rainfall, runoff and flooding data (Mays 2005; Bizier 2007). However, as the required records in the study area were unavailable, only the SWMM calibration was, hence, taken by using the 25-year and 1-h intensity-duration-frequency (IDF) curve of the rainfall of 41,111 stations, Samsen, Bangkok (http://bmm.doh.go.th/website/download), and later distributing it into the first-quartile storm hyetograph of the National Oceanic and Atmospheric Administration downloaded from www.weather.gov/media/owp/oh/hdsc/docs/Atlas14_Volume8.pdf (Vangelis *et al.* 2022) (see the fast rising and falling characteristics of the derived storm in the left-hand side of Figure 2). Also, one of the practical conditions that the surroundings were free from flooding was further assumed. Then, the roughness coefficients would be adjusted for the simulation of the flows such that the resulting inundation hotspots fairly matched the corresponding actual ones shown in Figure 1. The reasonable agreement between both of the hotspots finally gave the roughness coefficients of the pipes and the canals to be, respectively, 0.02 and 0.05, and resulted in the maximum free-outflow rate of 16.5 m^3/s.

2.3. The most critical condition of the model

As described earlier, the SWMM could simulate the university flooding that varies widely with the circumstance of nearby inundation and the type of storms striking. However, if we would like to use the SWMM as an impact assessment method of the interested climate change on flooding, it is, therefore, necessary to define the model for the flow simulation against only a condition that results in the most critical inundation. To find the worst flooding condition, we rationally expected that if the surroundings were flooded, the local inundation would be much more serious, as compared with that of the free-from-flooded neighbors. This is a consequence of the pumping capacity of 2 m^3/s that is considerably smaller than the maximum free-outflow rate of 16.5 m^3/s.

Following the rationale discussed above, the SWMM of the flooded surroundings was then used to further evaluate the effect of a few different storms. Such storms considered were the fast-increasing and decaying storm mentioned earlier, and the slow-rising and receding one (see their rainfall hyetographs in Figure 2). Results of the simulated inundation cases

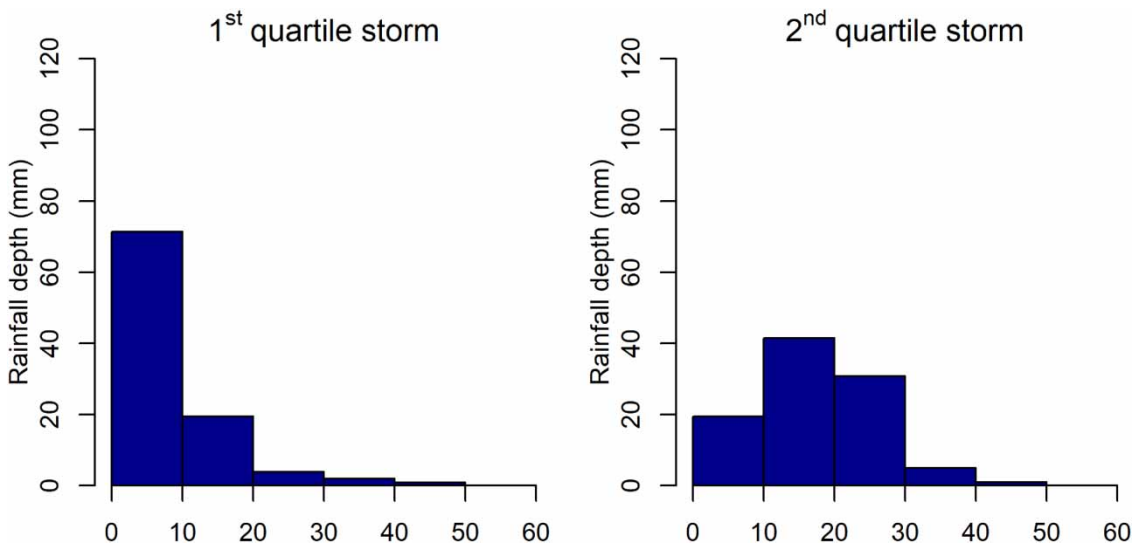

Figure 2 | The first- and second-quartile hyetographs of 25-year current storms for 1-h duration (Bangkok).

were later compared with those of the first-quartile storm for the missing nearby flooding condition. Particularly, the comparisons were performed using a total flooding hydrograph and its characteristics such as peak, volume and duration properties.

Figure 3 displays the total flooding hydrographs of the first- and second-quartile storms for the DS-TU with or without the inundated surroundings. Apparently, the hydrographs of the flooded surrounding condition are appreciably greater than the other, due to the much smaller pumping capacity, as expected. This identifies that the circumstance of the flooded surroundings is the condition for the most critical inundation in the university. However, the figure further demonstrates that the effect of the storms is much less important because the corresponding hydrographs of both considered storms are slightly different. That is, a slight delay in the hydrograph of the second-quartile storm from that of the first-quartile one is observed because of the gradually rising and falling characteristics of the storm. Also, another evidence of a marginal increase in the hydrograph peak attribute of such a storm is presented. This is perhaps because dynamic rainfall–infiltration interaction causes a little decrease in the actual capacity of soil moisture retention (Todisco *et al.* 2022; Guo Hongxiang *et al.* 2023).

In addition, the worst flooding circumstance classified is further verified by the referred characteristics of the hydrographs. Table 1 shows the normalized hydrograph peak, volume and duration of the flooded surrounding condition for the first- and second-quartile storms. Notice that the normalization is the ratio of the actual property considered over the corresponding base of the dry condition for the first-quartile storm. Evidently, the table indicates that the condition of the surroundings is still substantiated to be the most serious local flooding case because of the increase in the peak and volume characteristics by, at least, 25% from the conventional bases. Also, the table confirms the small effect of the different storms as the normalized properties of both storms are quite close to each other.

3. RESULTS AND DISCUSSION

Considering the SWMM of the most critical condition, the propagation of the extreme climate-intensifying rate for maximum rainfall in Bangkok (Worawiwat *et al.* 2021) into the flooding has been investigated. The examination used the super C–C rate of 14%/°C to increase the first-quartile 25-year existing storm (see Figure 2) over a few degree rise in local temperature (IPCC 2007, 2014). The time distribution of the derived storms followed the temporal pattern of the NOAA in which their

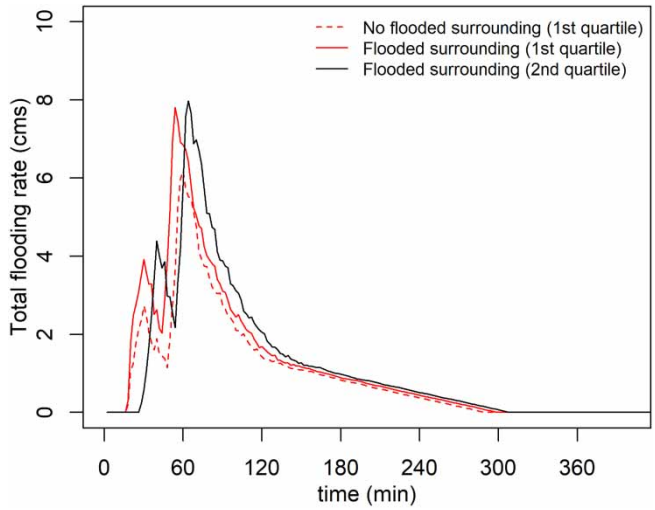

Figure 3 | The total flooding hydrographs of the first- and second-quartile storms for the DS-TU with or without the inundated surroundings.

Table 1 | Normalized hydrograph peak, volume and duration of the flooded surrounding condition for the first- and second-quartile storms

Storm	Peak	Volume	Duration
First quartile	1.26	1.26	1.04
Second quartile	1.29	1.26	1.03

Note: The normalization is the ratio of the actual property considered over the appropriate base of the dry condition for the first-quartile storm.

hyetographs were later modified by building an empirical dynamic relationship between the incremental storm rainfall and associated temperature into them (Trenberth 2011; Wasko & Sharma 2015).

Figure 4 presents the first-quartile dynamic storm of the extraordinary 14%/°C rate for the 1 °C rising temperature, and the increase of the higher-temperature storms from the 1 °C base. Obviously, the climate-intensifying storms would have their temporal patterns that dynamically grew across the time periods. For the maximum increase, its magnitude is much greater than those of the other time intervals, and its occurrence is located immediately at the start of the storms. The storm characteristics noted could lead us to expect that severe rainfall–flooding propagation might be possible.

Subsequently, the intensified storms were considered for the investigation of the extreme climate impact. Two types of examination depending on the clogging condition of the DS-TU were performed. First, if the DS was assumed to be fully opened, this investigation would be carried out for the pure climate effect. For the second examination, we have proposed the system to be partially clogged. Being the usual system condition but having been often ignored in most preceding studies, the proposal was, hence, examining the additional climate impact in association with the clogging level.

3.1. Fully opened system

In this case, the DS-TU is considered to be fully opened. The actual propagation of the super C–C 14%/°C rate was investigated by comparing it with that of the normal 7%/°C gradient for the rising temperatures. The comparison of the total flooding hydrographs for the extremely and usually intensifying rates is shown based on that of the current climate condition in Figure 5. It is obvious that the flooding hydrographs for these gradients generally increase from the considered base. Also, the growth of the steeper rate is seen to be larger than the increase of the milder one, and such a difference is observed to expand even more for the higher temperature.

Moreover, the increasing 14 and 7%/°C trends of hydrograph peak, volume and duration characteristics over the rising temperatures are further investigated in Figure 6. Table 2 summarizes the increase per degree Celsius of the properties. Evidently, they demonstrate that the increasing rate of the characteristics for the super C–C scaling would be linearly greater than that of the C–C slope, as one would normally expect, if the temperature was less than or equal to 2 °C. However, in case the temperature exceeded the 2 °C threshold, the drastically intensified rainfall would be severely propagating into the flooding, due to the exponential increase of such properties.

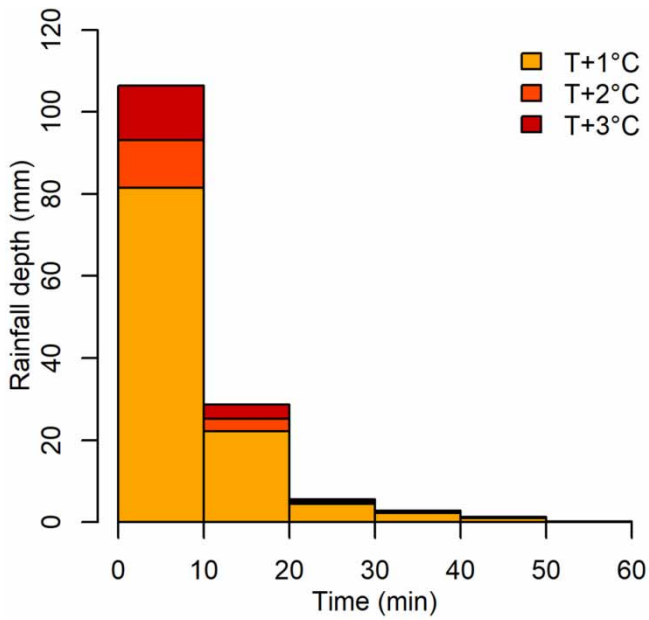

Figure 4 | The first-quartile storm of the extraordinary 14%/°C rate for the 1 °C rising temperature, and the net increase of the storms for the higher temperatures from the 1 °C base.

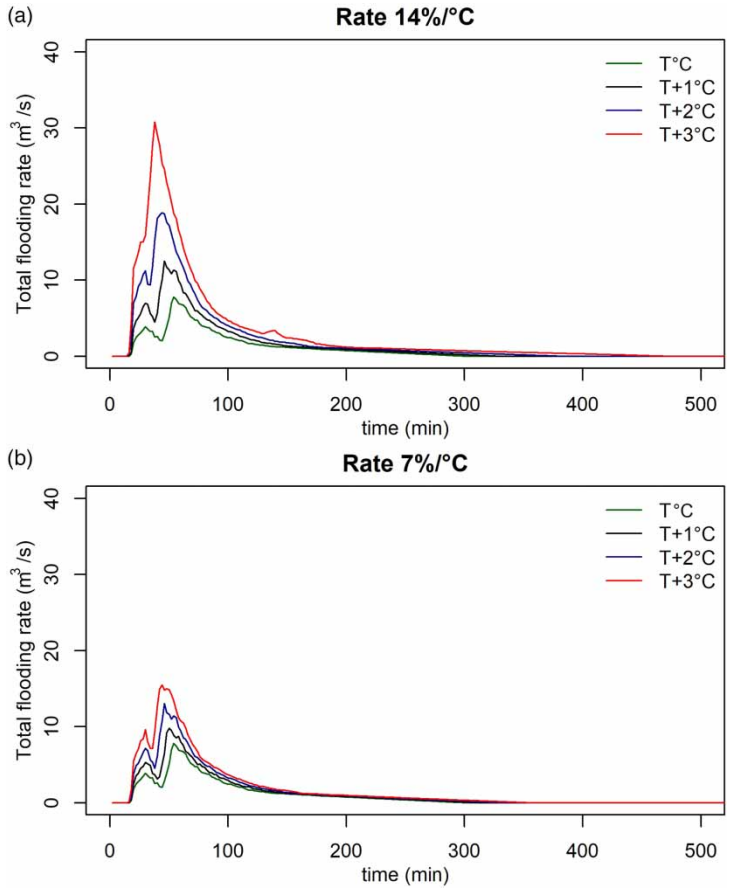

Figure 5 | Comparison of the total flooding hydrographs propagated by the climate-intensifying rate of (a) 14%/°C and (b) 7%/°C for a few degrees Celsius in rising temperature with that transmitted via the current climate condition.

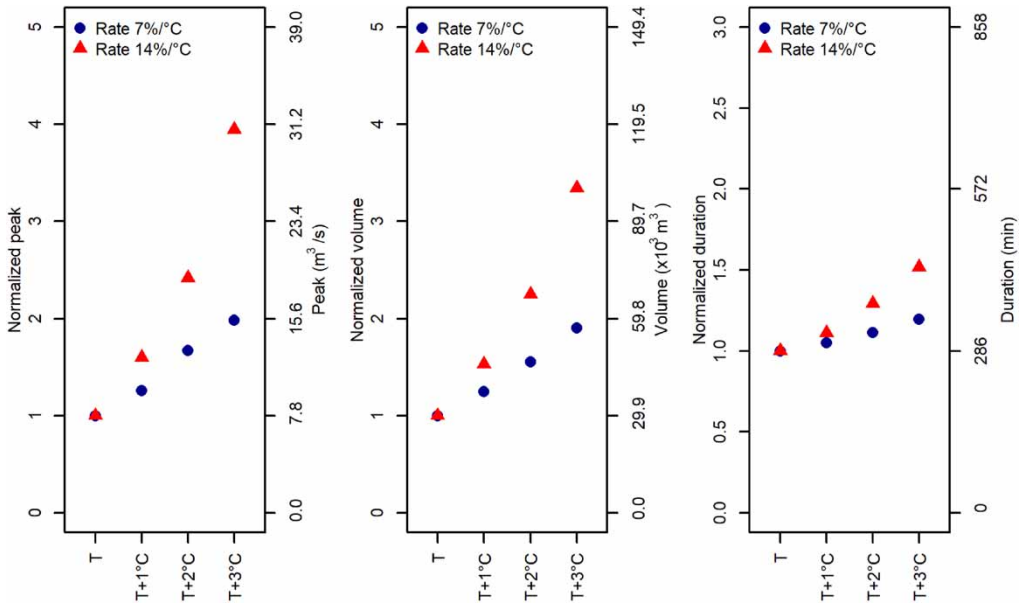

Figure 6 | Increasing 14 and 7%/°C trends of hydrograph peak, volume and duration characteristics over the rising temperatures. *Note*: The normalization is the ratio of the characteristic considered over the corresponding base of the present-day climate condition.

Table 2 | Increase per degree Celsius of the hydrograph peak, volume and duration properties

	Peak (m^3/s)		Volume ($\times 10^3$ m^3)		Duration (min)	
Rising temperature (°C)	**7%/°C**	**14%/°C**	**7%/°C**	**14%/°C**	**7%/°C**	**14%/°C**
0–1	2.02	4.69	7.36	15.82	14	32
1–2	3.21	6.37	9.14	21.51	18	52
2–3	2.45	11.95	10.5	32.75	24	64

3.2. Clogged system

In addition, the interested climate impact on the flooding was further examined through the DS-TU which was assumed to be partly obstructed. The low 30%, moderate 50% and high 70% clogging levels of the fully opened condition were then adopted (Worawiwat & Chaleeraktrakoon 2023). Their additions to the based case of the DS-TU without any blockage (e.g., see the previous subsection) were later investigated. Figure 7 presents the 14%/°C intensified hydrographs of the assumed clogging

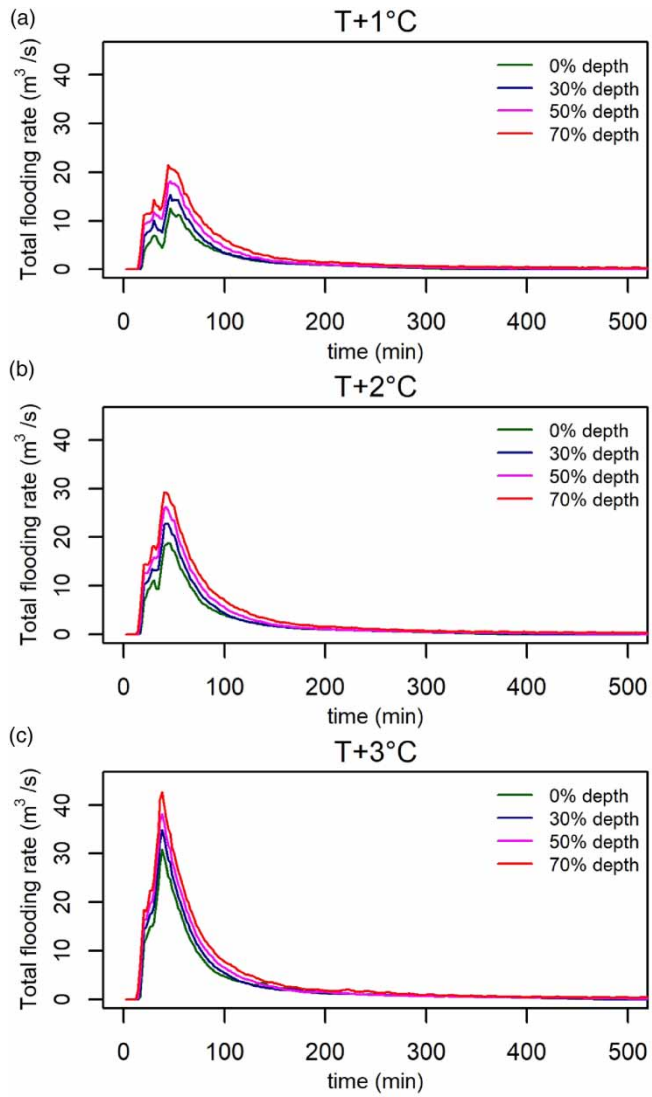

Figure 7 | The 14%/°C intensified hydrographs of the assumed clogging levels and the fully opened condition for (a) T+1°C, (b) T+2°C and (c) T+3°C in rising temperature.

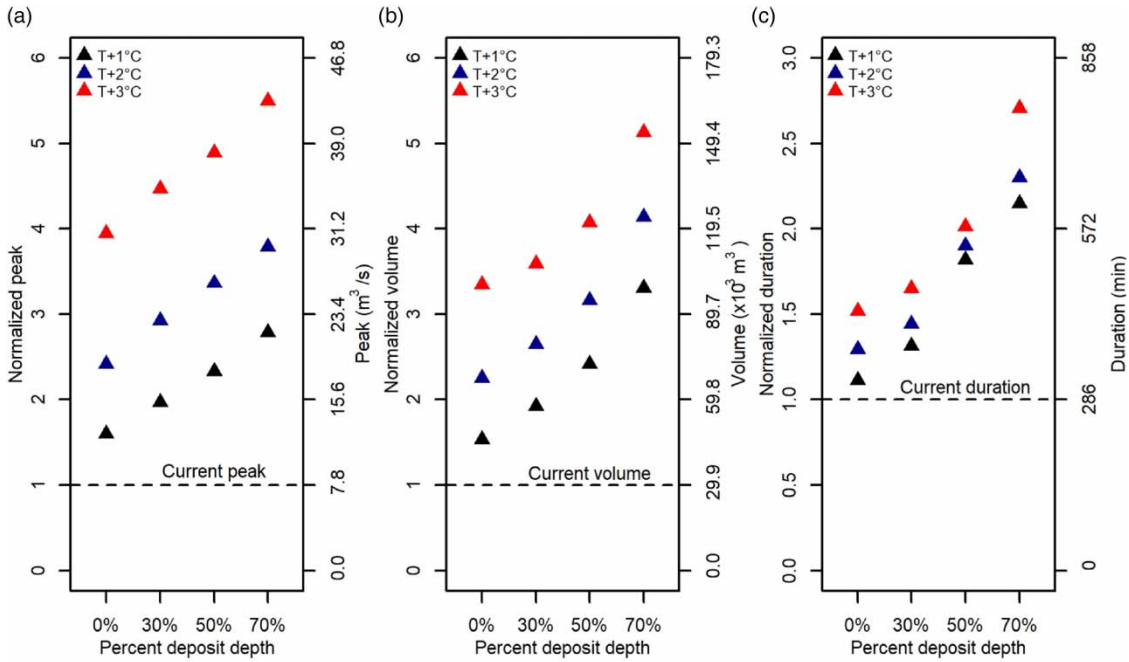

Figure 8 | Increasing tendency of (a) the hydrograph peak property, (b) the volume attribute and (c) the duration characteristic over several different clogging levels and various rising temperatures. *Note*: The normalization is the ratio of the characteristic considered over the corresponding base of the current climate condition.

Table 3 | Increase of the characteristics for each interval of successive clogging levels

	Peak (m^3/s)			Volume ($\times 10^3\ m^3$)			Duration (min)		
Clogging level	**T + 1 °C**	**T + 2 °C**	**T + 3 °C**	**T + 1 °C**	**T + 2 °C**	**T + 3 °C**	**T + 1 °C**	**T + 2 °C**	**T + 3 °C**
None to low (30%) level	2.84	3.98	4.03	11.73	11.97	7.26	58	42	38
Low to moderate (50%) level	2.87	3.40	3.33	14.70	15.26	14.45	144	132	104
Moderate to high (70%) level	3.54	3.30	4.74	26.67	29.17	31.56	94	114	198

levels that increase over the base of the fully opened condition for every a rise of a few degrees Celsius in local temperature. Such a growth is shown to vary directly with the clogging condition.

How the additional clogging effect transmitted into the hydrograph characteristics of the 14%/°C intensifying rate is presented in Figure 8 and Table 3. The figure displays the increasing tendency of the peak, volume and duration properties over several different clogging levels. The table classifies the growth of such properties for each interval of successive clogging conditions. These results show the importance of the proposed clogging problem to be jointly considered in the context of climate change because the proposal largely increases the climate-intensifying attributes. Moreover, they also demonstrate that this additional effect would be stable for every obstructing interval, like the result of the peak, but increasingly accelerating from the low-to-high condition, as shown for those of the volume and duration.

4. CONCLUSIONS

Currently managed flooding in Bangkok has been known to closely link with local maximum storm rainfall. This resulting linkage mainly causes the city inundation to certainly increase because the precipitation is usually intensified by the impact of global warming. Recent analysis of the climate-intensifying rate of the rainfall over each degree of rising temperature for the capital has found the gradient to be so extremely high (i.e., almost double the normal 7%/°C scaling) that none of the previous flooding investigations have taken it into account but most of the pasted studies have considered only the 7%/°C

scaling. Hence, understanding how the intense rainfall would propagate through a typical DS into flooding is necessary for sustainable management of the city inundation in the context of climate change.

Studying the propagation of the increased rainfall into the flooding necessitates the development of a general rainfall–runoff model that simulates the flows of the most critical flooding condition for a chosen DS representative in the capital. In this paper, the DS-TU in the flood-control polder was, at first, adopted and then modeled its rainfall–runoff relation using the traditional SWMM base. Calibration of the formulated SWMM was later performed by matching the simulated flooding hotspots resulting from the flows generated by the first-quartile 25-year current storm to the observed counterparts. Applying this developed SWMM for different storms and nearby flooding circumstances has identified the case of the inundated surroundings to be the most critical condition for the DS-TU. The condition gives the flooding hydrograph peak and volume that is approximately 25% greater than those of the other dry case.

The most critical SWMM has been later applied to assess how the extreme 14%/°C rainfall is propagating into flooding. The first-quartile hyetograph of a 25-year intense dynamic storm for a rise in temperatures ranging from 1 to 3 °C was then constructed for simulation of the flooding situations using the SWMM. Comparing the total flooding hydrograph and appropriate properties extracted (e.g., peak, volume and duration) of the increased storms with those of the normal 7%/°C counterparts have shown that the climb of the rising temperature above the threshold of 2 °C would lead the impact of the extreme rate to severely transmit into the flooding. This is because the intensified flooding characteristics are exponentially greater than those of the 7%/°C rate.

The impact of the 14%/°C intensifying rainfall has been further evaluated by considering a common clogging problem that is often ignored in previous studies. Accordingly, three different clogging levels (i.e., 30, 50 and 70% of the full openings) in the DS-TU were initially assumed, and the flooding situation of each considered level was subsequently simulated using the assessment SWMM. A comparison of these flooding results has demonstrated that taking the clogging problem into account additionally increases the flooding attributes of the extreme rate. The addition would be large and accelerating for the volume and duration properties if the clogging exceeded the low 30% level.

ACKNOWLEDGEMENTS

We would like to thank Thammasat University for supporting data on the study storm sewer system. Also, we appreciate two anonymous reviewers for their valuable comments regarding this paper.

AUTHOR CONTRIBUTIONS

AW contributed to programming software, and performing experimental cases. CC contributed to designing experiment, analyzing results, and writing and editing this paper.

FUNDING

Financial support from the Thailand Research Fund through the Royal Golden Jubilee Ph.D. Program (Grant No. PHD/0090/2560) is acknowledged. The authors also acknowledge Thammasat University for additional research funding in fiscal year 2023.

DATA AVAILABILITY STATEMENT

All relevant data are included in the paper or its Supplementary Information.

CONFLICT OF INTEREST

The authors declare there is no conflict.

REFERENCES

Agarwal, S., Roy, P. J., Choudhury, P. & Debbarma, N. 2021 Flood forecasting and flood flow modeling in a river system using ANN. *Water Practice and Technology* **16** (4), 1194–1205. doi:10.2166/wpt.2021.068.

Agarwal, S., Roy, P., Choudhury, P. & Debbarma, N. 2022 Comparative study on stream flow prediction using the GMNN and wavelet-based GMNN. *Journal of Water and Climate Change* **13** (9), 3323–3337. doi:10.2166/wcc.2022.226.

Agarwal, S., Mukherjee, D. & Debbarma, N. 2023a Analysis of extreme annual rainfall in North-Eastern India using machine learning techniques. *AQUA – Water Infrastructure, Ecosystems and Society* **72** (12), 2201–2215. doi:10.2166/aqua.2023.016.

Agarwal, S., Mukherjee, D. & Debbarma, N. 2023b Determination of annual rainfall in north-east India using deterministic, geospatial, and machine learning techniques. *Water Policy* **25** (12), 1113–1124. doi:10.2166/wp.2023.078.

Alexander, K., Hettiarachchi, S., Ou, Y. & Sharma, A. 2019 Can integrated green spaces and storage facilities absorb the increased risk of flooding due to climate change in developed urban environments? *Journal of Hydrology* **579**. doi:10.1016/j.jhydrol.2019.124201.

Anuthaman, S. N., Ramasamy, S., Ramasubbu, B. & Lakshminarayanan, B. 2023 Modelling and forecasting of urban flood under changing climate and land use land cover. *Journal of Water and Climate Change* **14** (12), 4314–4335. doi:10.2166/wcc.2023.164.

Arnbjerg-Nielsen, K., Willems, P., Olsson, J., Beecham, S., Pathirana, A., Bülow Gregersen, I., Madsen, H. & Nguyen, V. T. V. 2013 Impacts of climate change on rainfall extremes and urban drainage systems: A review. *Water Science and Technology* **68** (1), 16–28. doi:10.2166/wst.2013.251.

Ashish, S. 2013 *Impact of Climate Change on Urban Flooding in Sukhumvit Area of Bangkok*. Germany. doi:10.13140/RG.2.2.27839.00160.

Bizier, P. 2007 *Gravity Sanitary Sewer Design and Construction, ASCE Manual of Practice No. 60*. New York: ASCE.

BMA 2020 *Bangkok Flood Protection and Mitigation Planning 2020*. Thailand: Bangkok Metropolitan Administration, Bangkok.

Eamathicom, N. & Ounsiri, S. 2011 *Rough Survey of Flood Water Level After 2011 Mega Flooding at Thammasat University (Rangsit Campus)*. Thammasat University Library, Thammasat University, Pathum Thani.

Guo Hongxiang, Z. W., Cenliang, Z., Liyuan, C. & Zhiying, X. (2023) The impacts of Arctic climate and terrestrial environment changes on industries. *Chinese Journal of Polar Research* **35** (3), 460–478. doi:10.13679/j.jdyj.20220404.

Hamilton, D., Zhang, H. & Eccles, R. 2019 A review of the effects of climate change on riverine flooding in subtropical and tropical regions. *Journal of Water and Climate Change* **10** (4), 687–707. doi:10.2166/wcc.2019.175.

Haruyama, S. 1993 Geomorphology of the central plain of Thailand and its relationship with recent flood conditions. *GeoJournal* **31** (4), 327–334. doi:10.1007/BF00812782.

Hettiarachchi, S., Wasko, C. & Sharma, A. 2018 Increase in flood risk resulting from climate change in a developed urban watershed – The role of storm temporal patterns. *Hydrology and Earth System Sciences* **22** (3), 2041–2056. doi:10.5194/hess-22-2041-2018.

IPCC 2007 *Climate change 2007: synthesis report*. In: *Contribution of Working Groups I, II and III to the Fourth Assessment Report of the Intergovernmental Panel on Climate Change* (Core Writing Team, Pachauri, R. K. & Reisinger, A., eds). Geneva, Switzerland: IPCC.

IPCC 2014 *Climate change 2014: Synthesis report*. In: *Contribution of Working Groups I, II and III to the Fifth Assessment Report of the Intergovernmental Panel on Climate Change* (Core Writing Team, Pachauri, R. K. & Reisinger, A., eds).Geneva, Switzerland: IPCC.

Kiguchi, M., Takata, K., Hanasaki, N., Archevarahuprok, B., Champathong, A., Ikoma, E., Jaikaeo, C., Kaewrueng, S., Kanae, S., Kazama, S., Kuraji, K., Matsumoto, K., Nakamura, S., Nguyen-Le, D., Noda, K., Piamsa-Nga, N., Raksapatcharawong, M., Rangsiwanichpong, P., Ritphring, S., Shirakawa, H., Somphong, C., Srisutham, M., Suanburi, D., Suanpaga, W., Tebakari, T., Trisurat, Y., Udo, K., Wongsa, S., Yamada, T., Yoshida, K., Kiatiwat, T. & Oki, T. 2021 A review of climate-change impact and adaptation studies for the water sector in Thailand. *Environmental Research Letters* **16** (2). doi:10.1088/1748-9326/abce80.

Kongprasert, K. & Lekpungthiam, C. 2013 *Design of Drainage System in Thammasat University (Rangsit Campus)*. Thammasat University Library, Thammasat University, Pathum Thani.

Maimone, M., Malter, S., Anbessie, T. & Rockwell, J. 2023 Three methods of characterizing climate-induced changes in extreme rainfall: A comparison study. *Journal of Water and Climate Change* **14** (11), 4245–4260. doi:10.2166/wcc.2023.420.

Mays, L. W. 2005 *Water Resources Engineering*. Hoboken, NJ: Wiley.

Nguyen, T.-H. & Nguyen, V.-T.-V. 2020 Linking climate change to urban storm drainage system design: An innovative approach to modeling of extreme rainfall processes over different spatial and temporal scales. *Journal of Hydro-Environment Research* **29**, 80–95. https://doi.org/10.1016/j.jher.2020.01.006.

Nguyen, V. T. V., Nguyen, T. D. & Cung, A. 2007 A statistical approach to downscaling of sub-daily extreme rainfall processes for climate-related impact studies in urban areas. *Water Supply* **7** (2), 183–192. doi:10.2166/ws.2007.053.

Niazi, M., Nietch, C., Maghrebi, M., Jackson, N., Bennett, B. R., Tryby, M. & Massoudieh, A. 2017 Storm water management model: Performance review and gap analysis. *Journal of Sustainable Water in the Built Environment* **3**, 2. doi:10.1061/jswbay.0000817.

Qian, Q., Ketabdar, M., Jao, M. & Li, X. 2022 Modeling sediment load in storm drain system of southeast Texas coastal region. *Journal of Irrigation and Drainage Engineering* **148** (4), 04022004. doi:10.1061/(ASCE)IR.1943-4774.0001672.

Quang, C. N. X., Giang, N. N. H., Hoa, H. V. & Hung, P. Q. 2022 Effects of sediment deposit on the hydraulic performance of the urban stormwater drainage system. *IOP Conference Series: Earth and Environmental Science* **964** (1), 012020. doi:10.1088/1755-1315/964/1/012020.

Rossman, L. A. 2017 *Storm Water Management Model Reference Manual Volume II – Hydraulics*. Washington, DC: U.S. Environmental Protection Agency.

Rossman, L. A. & Huber, W. C. 2016 *Storm Water Management Model Reference Manual Volume I – Hydrology*. Washington, DC: U.S. Environmental Protection Agency.

Saito, N. 2014 Challenges for adapting Bangkok's flood management systems to climate change. *Urban Climate* **9**, 89–100. doi:10.1016/j.uclim.2014.07.006.

Todisco, F., Vergni, L., Vinci, A. & Torri, D. 2022 Infiltration and bulk density dynamics with simulated rainfall sequences. *Catena* **218**. doi:10.1016/j.catena.2022.106542.

Trenberth, K. E. 2011 Changes in precipitation with climate change. *Climate Research* **47** (1), 123–138. doi:10.3354/cr00953.

Vangelis, H., Zotou, I., Kourtis, I. M., Bellos, V. & Tsihrintzis, V. A. 2022 Relationship of rainfall and flood return periods through hydrologic and hydraulic modeling. *Water* **14** (22). doi:10.3390/w14223618.

Wasko, C. & Sharma, A. 2015 Steeper temporal distribution of rain intensity at higher temperatures within Australian storms. *Nature Geoscience* **8** (7), 527–529. doi:10.1038/ngeo2456.

Wibig, J. & Piotrowski, P. 2018 Impact of the air temperature and atmospheric circulation on extreme precipitation in Poland. *International Journal of Climatology* **38** (12), 4533–4549. doi:10.1002/joc.5685.

Wilby, R. L., Troni, J., Biot, Y., Tedd, L., Hewitson, B. C., Smith, D. M. & Sutton, R. T. 2009 A review of climate risk information for adaptation and development planning. *International Journal of Climatology* **29** (9), 1193–1215. doi:10.1002/joc.1839.

Worawiwat, A. & Chaleeraktrakoon, C. 2023 Dredging for existing storm sewer system: Short-term LID to mitigate flooding in Bangkok. *International Low Impact Development Conference* **2023**, 91–98. doi:10.1061/9780784485002.009.

Worawiwat, A., Chaleeraktrakoon, C. & Sharma, A. 2021 Is increased flooding in Bangkok a result of rising local temperatures? *Journal of Hydrology X* **13**, 100095. https://doi.org/10.1016/j.hydroa.2021.100095.

Zhou, Q., Leng, G. & Huang, M. 2018 Impacts of future climate change on urban flood volumes in Hohhot in northern China: Benefits of climate change mitigation and adaptations. *Hydrology and Earth System Sciences* **22** (1), 305–316. doi:10.5194/hess-22-305-2018.

First received 28 January 2024; accepted in revised form 18 August 2024. Available online 29 August 2024